Journal of Nuclear Materials 399 (2010) 266–274

Contents lists available at ScienceDirect

Journal of Nuclear Materials

journal homepage: www.elsevier.com/locate/jnucmat

Review

Creep behaviour of as received, aged and cold worked INCONEL 617 at 850 °C and 950 °C

S. Chomette [a,*], J.-M. Gentzbittel [a], B. Viguier [b]

[a] LITEN/DTH/LTH, CEA Grenoble, 17 Rue des Martyrs 38054, Grenoble Cedex 9, France
[b] Université de Toulouse, Institut Carnot CIRIMAT, ENSIACET-INPT, 4 Allée Emile Monso, BP 44362 31432 TOULOUSE Cedex 4, France

ARTICLE INFO

Article history:
Received 15 May 2009
Accepted 27 January 2010

Keywords:
Inconel 617
Creep
High temperature
Ageing treatment
Cold work
Microstructure

ABSTRACT

The effect of initial microstructure on alloy 617 creep behaviour has been investigated at 850 °C and 950 °C. The solution treated material shows non-classical creep behaviour at both temperatures with a strain rate drop at the beginning of the tests followed by a creep rate increase to a plateau before the onset of the tertiary creep. The intragranular secondary carbides which precipitate early at test temperature are responsible of the strong initial hardening effect by pinning the dislocations. This effect is overpassed during the thermo mechanical ageing of the alloy which induces growth of these carbides. Prior 1000 h thermal ageing at the temperature test totally removes the strain rate drop and reduces the lifetime. The intragranular microstructure has evolved thanks to the prior thermal ageing before the creep tests. Microstructural examinations also show the presence of grain boundary migration and recrystallization in the material during creep tests of the as received and aged materials. Preliminary cold work treatment highly reduces the strain rate of Inconel 617 and enhances the lifetime at 850 °C while the opposite is observed at 950 °C.

Contents

1. Introduction

Inconel 617 is a nickel–chromium–cobalt–molybdenum superalloy with a good combination of thermal stability, corrosion and oxidation resistance and creep resistance up to 1000 °C. This alloy is expected to be used as the material for hot ducts and for the intermediate heat exchanger between the primary and the secondary coolant circuits in the Very High Temperature Reactor (VHTR). The nominal operation conditions of the exchanger, called IHX, will be in the temperature range of 800–1000 °C a pressure difference of 80 bar (8 MPa) for more than 100,000 h. As so long creep tests cannot be experimentally realized, an estimation of the creep life could be obtained with models based on laboratory experiments done under higher stresses. The effect of preliminary thermo mechanical treatments have also to be taken into consideration in order to complete the Inconel 617 creep data base. MC, M_6C

* Corresponding author. Tel.: +33 438 783 256; fax: +33 438 789 501.
E-mail addresses: sebastien.chomette@orange.fr (S. Chomette), jean-marie.gentzbittel@cea.fr (J.-M. Gentzbittel).

0022-3115/$ - see front matter © 2010 Elsevier B.V. All rights reserved.
doi:10.1016/j.jnucmat.2010.01.019

and $M_{23}C_6$ carbide types are present in the as received condition or after thermal treatments on the Inconel 617 [1–3], although this alloy is classified as a solid-solution strengthened one. Several results show that this precipitates have an influence on the creep properties of alloy 617 [2].

In the present work, we first looked at the microstructure evolution during heat treatments at 850 °C and 950 °C. Creep properties of Inconel 617 have been studied at 850 °C and 950 °C on the as received material for different stress levels and under different atmospheres. The influence of heat treatments as well as cold work prior to creep tests is also investigated. The results are discussed in terms of creep parameters and microstructural evolution of the alloy.

2. Experimental procedures

The Inconel 617 was supplied by Special Metals in a hot rolled bar form of 50 mm in diameter. The as received material has been solution annealed in shop at 1177 °C during 63 min and water quenched. The chemical composition of this bar is shown in Table 1. Fig. 1 shows the microstructure of the as received Inconel 617. It is made of equiaxed grains with a size of 270 μm (ASTM 5). The precipitation of the Inconel 617 in the as received condition consists in primary carbides with an average size of 5 μm (Ti(C, N) and M_6C Mo rich precipitates), uniformly distributed in the matrix as shown in Fig. 1. Few $M_{23}C_6$ Cr rich secondary carbides have also been observed within the grains and in some grain boundaries showing that the annealing treatment was not sufficient to dissolve all this secondary precipitates, as indicated by Mankins et al. [1].

The thermal ageing treatments from 1 h to 100 h at 850 °C and 950 °C for microstructural examination were done in air. In this case, samples were introduced in hot pre-heated furnaces. Therefore, the ageing duration was not influenced by the initial elevation of temperature of the furnace. For 1000 h ageing at both temperatures, the samples were put in cold furnaces working in an argon atmosphere (samples for microstructural examination) or in air (creep specimens). The furnaces were then warmed-up. The samples were all furnace cooled.

Cylindrical specimens with a gauge diameter of 5 mm and a 30 mm gauge length for tests in air and with a gauge diameter of 6 mm and a 25 mm length for tests under vacuum were machined from the as received and aged alloy 617 rod. In both cases, the loading direction corresponds to the bar axis. The creep tests in air were done on MAYES creep machines with a load capacity of 30 kN and equipped with resistive furnaces. The vacuum creep test machine with a 2 kN load capacity works under high vacuum (10^{-4} Pa) with a resistive furnace. In both cases, the specimen elongation is measured with LVDT type sensors. For air tests, these sensors are directly connected to the specimen gage, while for vacuum testing the displacement between fixed frame and the mobile tie rod is measured. Mechanical loading is insured by dead weights which are manually gently set on in order to get a mean loading rate of about 1.4–2 $N.s^{-1}$.The tests are performed at 850 °C or 950 °C under constant load. The heating rate was fixed at 10 °C min^{-1}. The tests started 1 h after the setpoint temperature was reached in order to stabilize the whole experimental apparatus. Table 2 lists the different conditions and rupture time of the creep tests. The creep tests after thermal ageing were done at ageing temperature. Cold work creep specimens were submitted to a tensile strain of 20% at room temperature with a strain rate of 5×10^{-4} s^{-1} before creep tests. It has been verified on interrupted creep test that strain is uniform on all the gage length up to the end of the secondary creep stage. Therefore, the creep curves are reported in terms of true strain and true strain rate. This representation is less valid for the end of the creep curve (tertiary stage).

The observation of the aged samples was made in a plan normal to the axis of the bar and the study of the creep specimens is done in a plan parallel to this axis (load direction). In all cases, the samples were cut and coated in resin. They were mechanically polished with SiC paper to grade 2400 and finished with 3 μm diamond paste. Finally, the specimens were electrochemically etched at 2 V in a 100 mL of HCl + 5 mg of oxalic acid solution.

Table 1
Chemical composition of the 50 mm in diameter hot rolled bar supplied by special metals (wt.%).

Ni	Cr	Co	Mo	Ti	Al	C
Bal.	21.33	12.15	9.21	0.41	0.92	0.059

3. Results

3.1. Microstructure evolution during unstressed ageing treatments

Fig. 2 shows the typical microstructure of Inconel 617 after ageing treatments of 1 h to 1000 h at 850 °C. After 1 h at 850 °C, the etching treatment has revealed the slip lines in all the grains. Cr rich $M_{23}C_6$ carbides are observed in grain boundaries and twins habit planes. Numerous fine Cr rich $M_{23}C_6$ precipitates have appeared on slip lines after 10 h of heat treatment at 850 °C. Even if some $M_{23}C_6$ carbides were observed in the as received material, these fine precipitates were not present in the as received condition. The thickness of the intergranular carbides increases while it does not evolve in twins habit planes after 10 h. The intragranular precipitates are then slightly less numerous but thicker after thermal

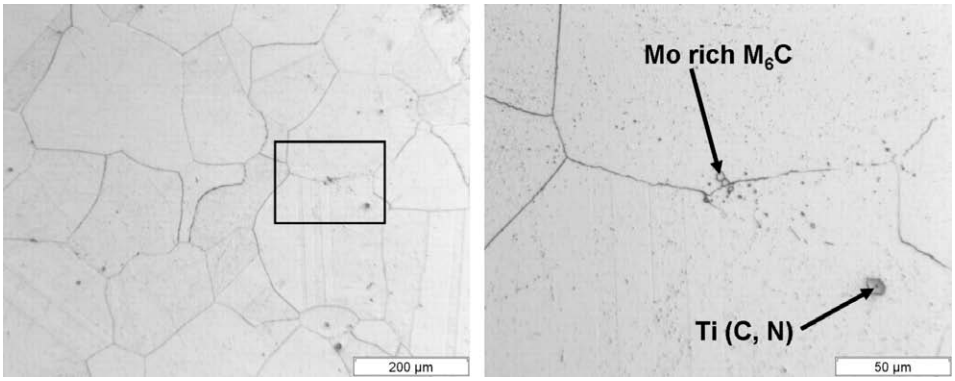

Fig. 1. Microstructure of the as received Inconel 617.

Table 2
Creep test conditions and results.

Temperature (°C)	Stress (MPa)	Environment	Initial thermo mechanical treatments	Test duration (h)
850	80	Vacuum	AR	480
850	80	Air	AR	400
850	70	Vacuum	AR	1170
850	70	Air	AR	Stop at 500
850	70	Air	Aged 1000 h/850 °C	970
850	70	Air	20%cold worked	2340
850	55	Vacuum	AR	5570
950	35	Vacuum	AR	1630
950	30	Vacuum	AR	3450
950	30	Air	AR	3950
950	30	Altered vacuum	AR	1120
950	30	Vacuum	Aged 1000 h/950 °C	1280
950	30	Air	20%cold worked	300
950	20	Vacuum	AR	13,940

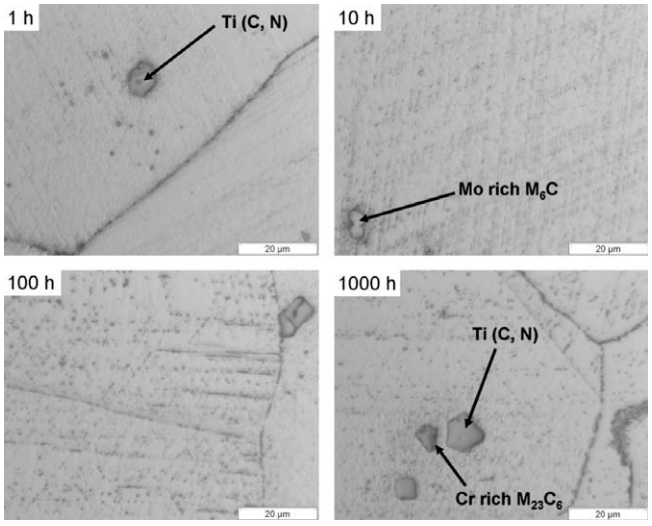

Fig. 2. Evolution of the microstructure of Inconel 617 after ageing treatments of 1–1000 h at 850 °C.

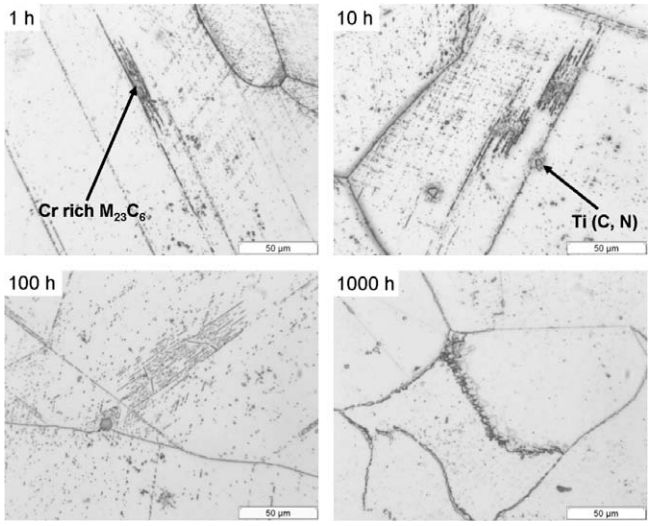

Fig. 3. Evolution of the microstructure of Inconel 617 after ageing treatments of 1–1000 h at 950 °C.

ageing for 100 h than for 10 h, which reveals the carbide coalescence. Fine carbides still exist on slip lines after 1000 h, but less numerous than for shorter heat treatments. Some large intragranular Cr rich $M_{23}C_6$ have formed in grains but also around primary carbides (Ti(C, N) and Mo rich M_6C) corresponding to their decomposition as shown in Fig. 2. The thickening of the intergranular carbides continues from 100 h to 1000 h but the thickness of twins habit planes carbides is the same as it was after 1 h ageing treatment.

The evolution of intragranular secondary carbides is faster at 950 °C than at 850 °C as shown in Fig. 3. Indeed, after 1 h of ageing treatment at 950 °C, few Cr rich $M_{23}C_6$ precipitates are observed on slip lines. The number and the size of these carbides do not seem to change up to 100 h of ageing. After 1000 h at 950 °C, only a few big $M_{23}C_6$ are still present in grains. Mankins et al. [1] explain that the nucleation rate of secondary carbides reaches a maximum near 871 °C and decreases for higher temperatures for which diffusion and thus growth is favoured. This is in agreement with our observation that the $M_{23}C_6$ precipitates are more numerous at 850 °C than at 950 °C. Concerning grain boundaries, the coarsening of intergranular precipitates leads to the formation of big compact walls made of globular carbides after 1000 h at 950 °C that can be seen in Fig. 3. In comparison with 850 °C, nearly continuous carbide walls are observed in twin habit planes for aged samples at 950 °C.

A singular precipitation is observed during ageing at 950 °C that does not appear at 850 °C. Lamellar carbides precipitate on both sides of twins ends in all grains after 1 h of ageing as shown in Fig. 3. The dissolution of these precipitates can be observed from 10 h of heat treatment to eventually disappear after 1000 h. The fact that these carbides appear during ageing at 950 °C show that they are secondary carbides (Cr rich $M_{23}C_6$), but further analysis are needed to conclude.

Kihara et al. [2] explain that intragranular carbides are metastable precipitates and dissolved with ageing time at 1000 °C. The more stable intergranular carbides grow thanks to this dissolution. However, the microstructural examination of thermal aged samples at 850 °C and 950 °C does not show a preferential dissolution of intragranular carbides near the grain boundaries.

The microstructural evolution of the Inconel 617 can be related to the evolution of hardness after ageing treatments at 850 °C and 950 °C, summarised in Fig. 4. At both temperatures, the hardness increase starts early during the ageing treatments as this increase is observed after 1 h. It seems that the intragranular carbides on slip lines appear before 1 h even if they are not observed on optical micrographs. The peak of hardness appears in the first few ten hours of ageing treatment when the intragranular $M_{23}C_6$ precipitates on slip lines are the most numerous. The hardness evolution after 1000 h is very limited so the most important microstructural changes can be considered to occur before 1000 h of heat treat-

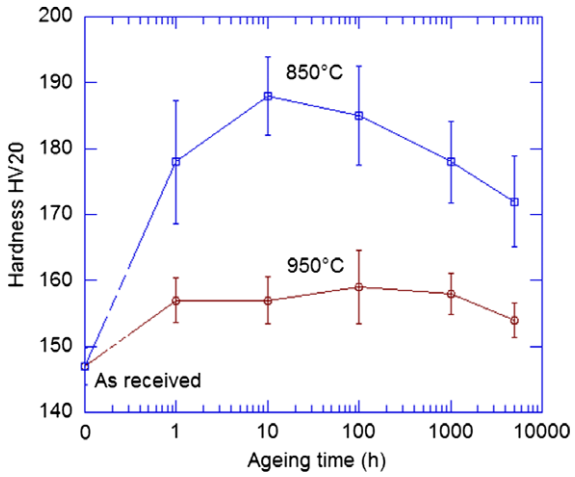

Fig. 4. Inconel 617 hardness evolution with ageing time at 850 °C and 950 °C.

ment. The higher hardness peak for ageing treatments at 850 °C than at 950 °C can be explained with the fact that nucleation is favoured at 850 °C while diffusion is favoured at 950 °C [1]. Wu [3] has also observed a hardness peak for short duration ageing treatments between 700 °C and 800 °C in the case of the CCA 617 (Chemical Controlled Alloy 617), alloy derived from alloy 617 with a specific chemical composition.

3.2. As received creep behaviour

The creep curves of as received Inconel 617 samples tested to rupture at 850 °C (55–80 MPa) and 950 °C (20–35 MPa) are shown in Fig. 5. Fig. 5a and 5c shows that creep tests made in air or under high vacuum at 850 °C under a stress of 80 MPa and at 950 °C under 30 MPa give nearly the same curves and rupture time. Hosoi Abe [4] find the same results when they compare creep tests on Inconel 617 at 1000 °C under 35 MPa in air and under a pressure of 1.2×10^{-3} mbar. They also show that this alloy exhibits a minimum creep rupture time between these two pressures at about 1.3×10^{-2} mbar at 1000 °C. Several tests under altered vacuum at 950 °C have shown reduced rupture life and an enhanced strain rate, when compared to high vacuum tests and to all air tests at the same temperature. The curve of one of these tests under altered vacuum is compared to another test done under high vacuum in Fig. 5e and f. The observation of the surface of all the altered vacuum samples shows an oxide scale thinner than the as received specimen crept in air, proof of partial vacuum during these tests. Unfortunately, the relative pressure was not recorded, but it seems that these tests were done under a pressure near the minimum of rupture life at 950 °C like Hosoi and Abe [4] show at 1000 °C.

Concerning the description of as received Inconel 617 creep curves, the shape of these curves at 850 °C and 950 °C is very singular. At 850 °C, a quick examination of the true strain versus time curves shows a near typical shape with a primary, secondary and tertiary stage (Fig. 5b). Schubert et al. [5] make the same description of Inconel 617 creep curves at 850 °C under stresses between 30 MPa and 56 MPa. However, the analysis of the strain rate versus strain curves shows that for all stresses, a minimum strain rate is observed at the end of the primary creep stage followed by a strong increase of the strain rate until a strain of about 3%. For higher strain under high stresses (70 MPa and 80 MPa), the strain rate increases more slowly until the rupture of the sample. Under low stresses (55 MPa), the strain rate decreases slightly until the beginning of the tertiary creep stage. The particular point at a strain level of 3% at 850 °C seems to be the end of the transition between two different domains: domain I just after the primary regime composed of the minimum creep rate level and domain II considered to be the secondary regime. The shape of Cook's [6] creep curves at 850 °C in air under 45 MPa and 48 MPa is similar to the 850 °C/55 MPa creep curve shape presented in Fig. 5a with a minimum creep rate followed by an increase of strain rate that seems to stop too at a strain of approximately 3%. However, Cook's [6] creep curves do not show primary creep stage.

As for the creep test at 850 °C under 55 MPa, the study of the creep curves at 950 °C summarised in Fig. 5c and d shows two different regions between the primary and the tertiary creep stage. The first region corresponds to a very fast drop of the strain rate down to a minimum value called here minimum creep rate which depends on stress (10^{-9} s^{-1} for 20 MPa) followed by a sudden increase of the strain rate. Following this downward peak, a kind of plateau is observed with a slight decrease of the strain rate. Again, the level of the plateau which will be labelled secondary creep rate depends on the applied stress. According to the literature, only Schneider et al. [7] relate the same creep behaviour for the Inconel 617 at 950 °C and this particular creep curves shape has also been observed at 1000 °C for another Ni based alloy by Kurata et al. [8] (Hastelloy XR). One can notice that the end of the transition from one domain to the other occurs at a strain of 2% for all stresses. The same result is shown in Schneider et al. [7] strain rate versus strain curves. For further comparison, the strain rate at a strain of 3% at 850 °C and 2% at 950 °C are considered to be the secondary creep rate.

The as received specimens crept at 850 °C under 70 MPa and at 950 °C under 35 MPa have been chosen in order to compare the microstructure of aged and crept samples with approximately the same duration of thermal exposure (1000 h). After rupture at 850 °C under 70 MPa, a few migrations of grain boundaries and twins are observed in the material (Fig. 6). These migrations do not appeared for heat treatments up to 1000 h at 850 °C (Fig. 2) but the crept sample shows a less important carbide precipitation in twins habit planes than in grain boundaries as shown in Fig. 6a. Consequently, the movement of habit planes is easier than grain boundaries during creep at 850 °C thanks to a higher distance between precipitates. Recrystallization is also observed during creep at 850 °C. Recrystallized zones are found along grain boundaries with the formation of multiple fine grains containing twins which are not observed for only aged specimens up to 1000 h. Numerous big creep voids are observed all along the gage length after rupture. Intragranular Cr rich $M_{23}C_6$ are still observable on slip lines and grain boundaries in old grains of the 850 °C crept sample. However, the areas swept by the migrated boundary and the recrystallization zones are nearly free of carbides as are the new grain boundaries. The crept sample interrupted after 500 h already shows grain boundary migration and recrystallization as shown in Fig. 6b. The recrystallized zones are only located at grain triple junctions but also at grain boundaries and twins habit planes junctions. The recrystallization is limited to one or two grains. Concerning grain boundary migration, the observations show that no important evolution seems to occur between 500 h and the rupture during creep. Some voids are also observed as shown in Fig. 6b even if the tertiary creep regime does not seem to be reached after 500 h under these conditions.

The final rupture of the samples seems to originate from different mechanisms depending on the creep temperature. Indeed, for the specimens crept at 850 °C, one can observe a uniform and moderated reduction in area on the whole gage length as seen in Fig. 7. Whereas for 950 °C tests, necking is clearly observed with a localized deformation during the tertiary creep stage. Fig. 8 shows the microstructure of a ruptured 950 °C/35 MPa sample. Far from the facture region, the precipitation in old grains and in grain boundaries is the same as only aged sample during 1000 h at 950 °C.

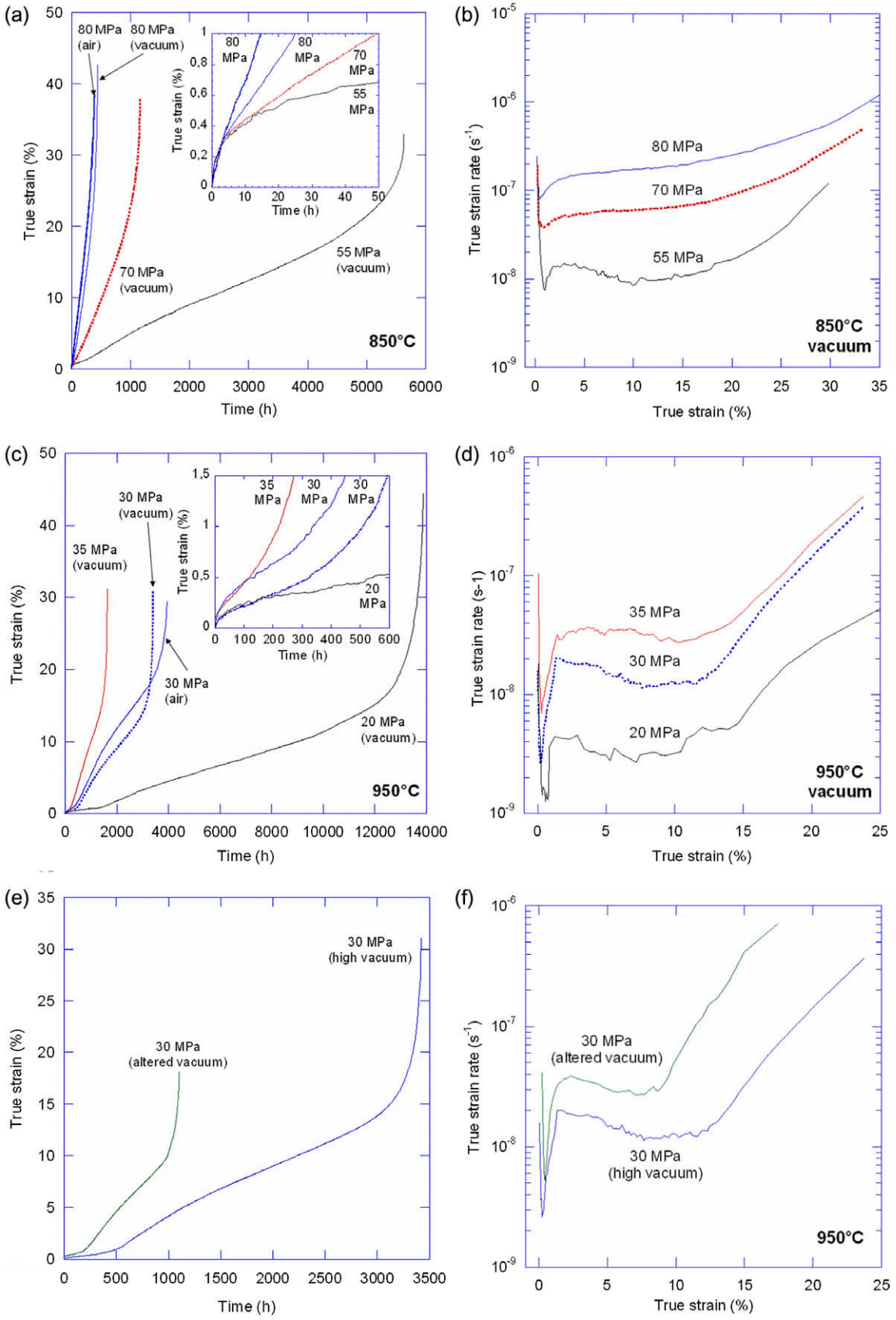

Fig. 5. Creep curves for samples of as received Inconel 617: (a) true strain versus time at 850 °C, (b) true strain rate versus true strain at 850 °C, (c) true strain versus time at 950 °C, (d) true strain rate versus true strain at 950 °C, (e) true strain versus time at 950 °C under high and altered vacuum and (f) corresponding true strain rate versus true strain.

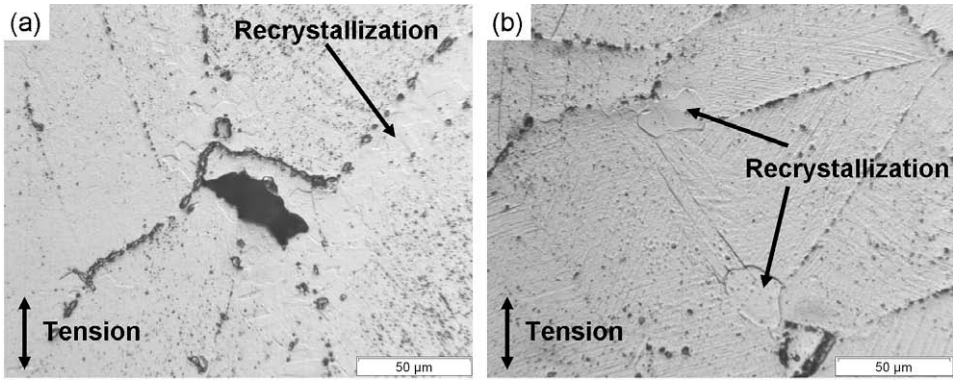

Fig. 6. Microstructure of as received Inconel 617 samples after rupture (a) and interrupted after 500 h of creep test (b) at 850 °C under 70 MPa.

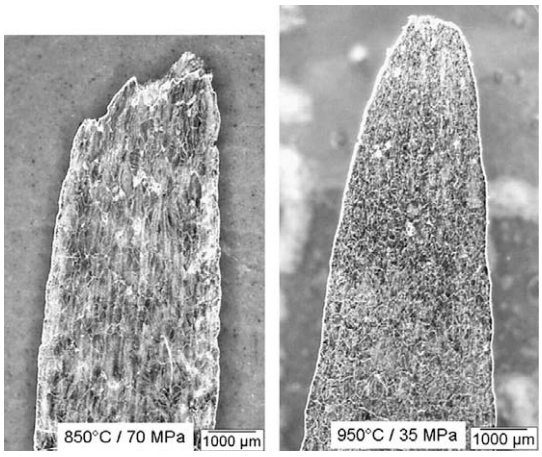

Fig. 7. Comparison of ruptured samples reduction in area between 850 °C/70 MPa and 950 °C/35 MPa.

The microstructure of the sample shows larger recrystallized grains at triple junctions compared to the sample tested at 850 °C under 70 MPa. Some boundary migrations are also observed. Near the rupture zone, the microstructure is totally remodelled with a widespread recrystallization and no new intragranular precipitation. The remaining precipitates in this zone are primary M_6C and Ti (C, N) carbides and old grain boundary $M_{23}C_6$ carbides that can be found in new grain boundaries or in grains. It seems that the recrystallization impedes part of the damage as very few creep voids are observed all along the gage length. The same microstructural differences between the fracture region and far from it are also observed in creep tests at 1000 °C on as received Hastelloy XR [8].

3.3. Creep behaviour after ageing and after cold work

As all the major microstructural changes happened quickly during heat treatments (§ 2.1), 1000 h has been chosen as ageing time . The microstructure of Inconel 617 can be considered with no significant modifications for longer durations. Creep tests have been made after these ageing treatments to determine the effect of carbides on Inconel 617 creep response. The creep curves of these samples are compared to the as received ones tested in the same conditions in Fig. 9.

Concerning the creep behaviour of aged Inconel 617, the preliminary heat treatments have major influences on creep behaviour, especially at 950 °C. Indeed, preliminary ageing treatment reduces a little the lifetime at 850 °C/70 MPa but highly reduces it at 950 °C/30 MPa. It also reduces elongation in the same way. According to these results, a preliminary ageing treatment of 1000 h is more deleterious at 950 °C than at 850 °C on creep response. Concerning the creep curves, the shape shows an important primary creep stage that ends at large strain level immediately followed by the tertiary creep regime as shown in Fig. 9. The two domains I and II observed between primary and tertiary regimes on the as received material are no more visible after the initial heat treatments. The same curves shape is observed by Schneider et al. [7] after long ageing time at 950 °C on Inconel 617 creep curves at the same temperature under low stresses and for all ageing times under high stresses.

The microstructure of the 1000 h/950 °C aged creep specimen after rupture has been examined to determine the ageing effects

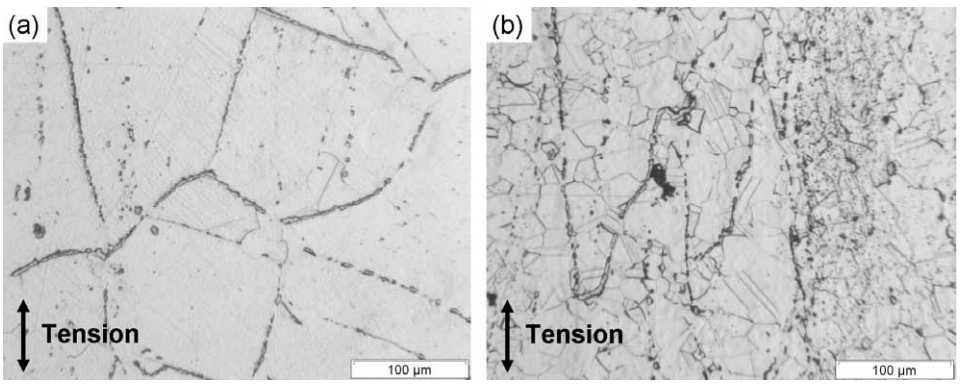

Fig. 8. Microstructure of an as received Inconel 617 creep sample after rupture at 950 °C under 35 MPa: (a) low reduction in area far from the rupture zone, and (b) high reduction in area near the rupture zone.

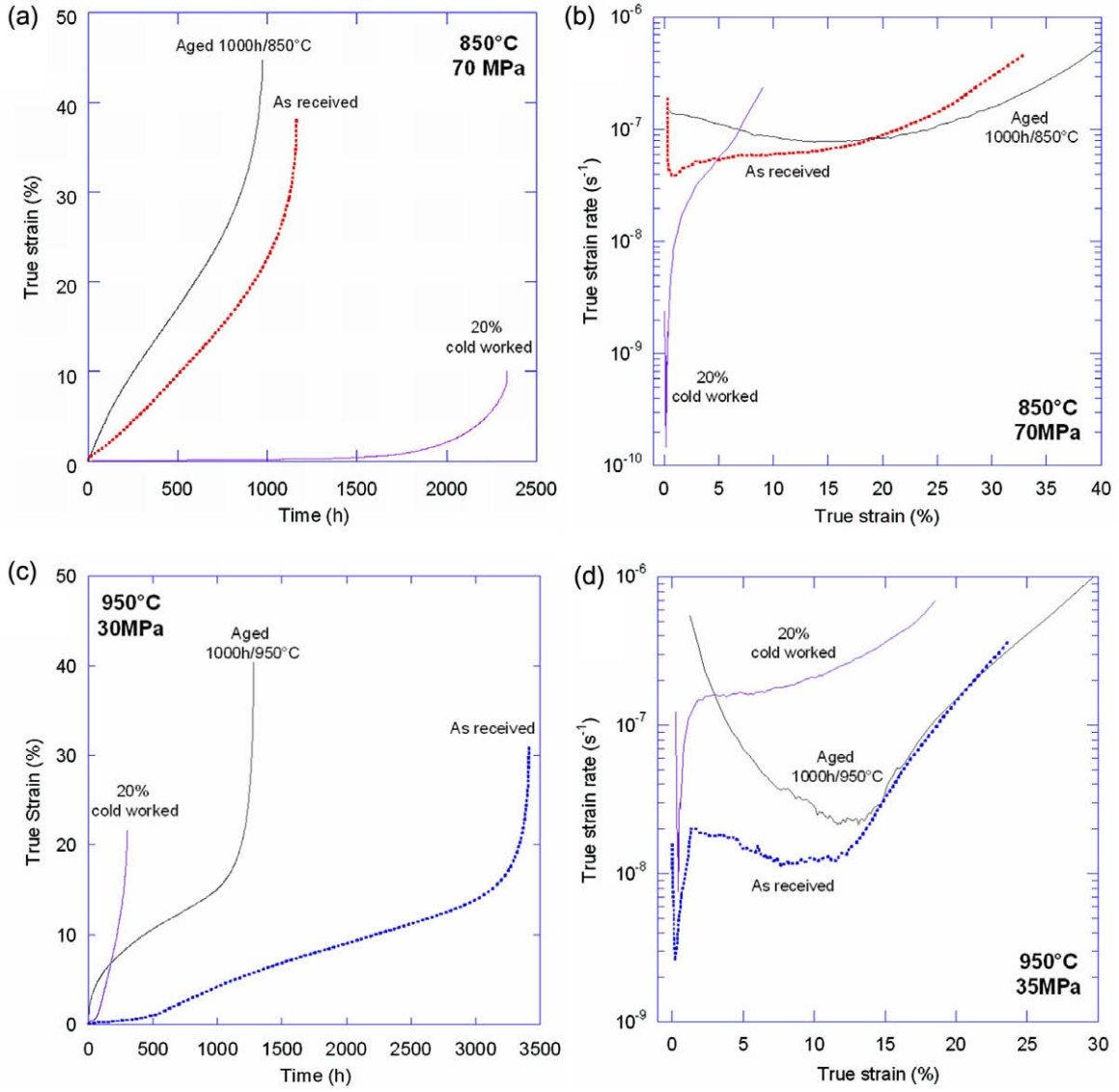

Fig. 9. Comparison of creep curves for samples of as received, aged 1000 h at creep temperature and 20% cold worked Inconel 617: (a) true strain versus time at 850 °C under 70 MPa, (b) true strain rate versus true strain at 850 °C under 70 MPa, (c) true strain versus time at 950 °C under 30 MPa, (d) true strain rate versus true strain at 950 °C under 30 MPa.

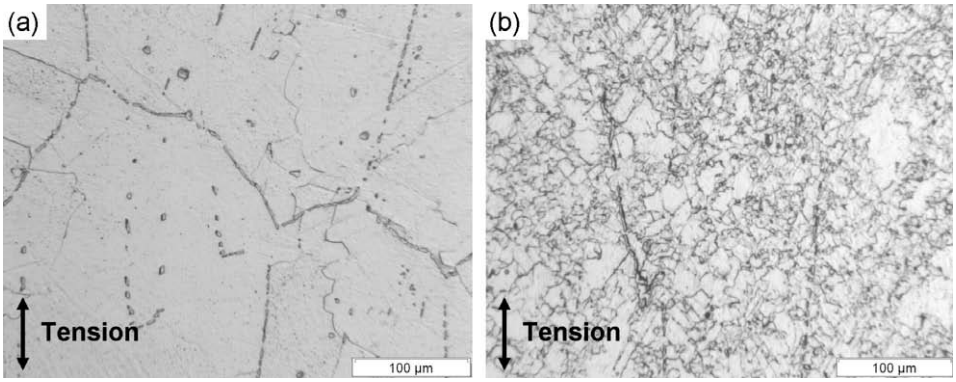

Fig. 10. Microstructure of the 1000 h/950 °C aged Inconel 617 creep sample after rupture at 950 °C under 35 MPa: (a) low reduction in area far from the rupture zone, and (b) high reduction in area near the rupture zone.

during test. This microstructure is shown in Fig. 10. The reduction in area of the aged sample is about 90% and localized what implies different microstructures far from and near the rupture zone as for the as received material tested at 950 °C. Far from the fracture region, no precipitation differences are observed between the as received creep and the aged and crept samples. However, the

amplitude of grain boundary migration and the size of new grains formed by recrystallization are more important in the aged ruptured specimen as shown in Fig. 10a. The intragranular carbides dissolved in aged specimen could not reduce the size of new grains by pinning their boundaries as they do in the as received material. Near the rupture zone, a complete recrystallization of the sample is observable with quite smaller grains than in the as received material crept at 950 °C as shown in Fig. 10b.

According to Fig. 9a, a 20% cold work on Inconel 617 considerably reduces the elongation to rupture and strongly increases lifetime for creep tests at 850 °C as compared to as received material. However, at 950 °C, the elongation for the same cold worked is only slightly reduced when compared to the as received material and the lifetime is drastically reduced as seen in Fig. 9c. Cook [6] and Mino et al. [9] show the same results for Inconel 617 for 5% to 20% cold works at 850 °C and for 17% cold work at 1000 °C respectively. Hastelloy XR shows the same trends at 850 °C and 950 °C with approximately the same levels concerning elongation to rupture and lifetime [8]. Concerning the strain rate versus strain curves shown in Fig. 9b, it appears that except for the strain rate drop which is two orders of magnitude lower, the strain rate at 3% of strain is equivalent to the as received tests one at 850 °C. As the most important part of the creep test at 850 °C after cold work is composed by the domain I described above (Fig. 9a), it seems that the cold work has stabilised this domain. On the contrary, the domain I is unstable at 950 °C as this phase is short as shown in Fig. 9c when compared to the as received material while the domain II is enhanced by the cold work. The strain rate of this domain is one order of magnitude higher for the cold worked test than for the as received one at 950 °C (Fig. 9d).

4. Discussion

4.1. Creep behaviour of Inconel 617

Before creep tests, the initial annealing treatment at 1177 °C does not dissolve all the secondary carbides [1]; they are observed in the as received material. This precipitate growth generates dislocations on which new Cr rich $M_{23}C_6$ carbides could precipitate during the subsequent temperature exposure [1]. In the tests performed for this study, the precipitation of secondary carbides starts on slip lines during the 1 h stage of temperature stabilisation before creep tests start. In fact, the microstructure of the creep samples is not the as received one but the microstructure of the 1 h aged samples shown in Figs. 2 or 3 at the beginning of the tests. Therefore, some Cr rich $M_{23}C_6$ carbides have already precipitated on slip lines when the as received material creep tests start and hardened the matrix by pinning dislocations. This precipitation continues during ten hours after the beginning of the tests. The large amount of intragranular secondary carbides limits the dislocation mobility in the as received material. This phenomenon explains the initial strain rate drop in the beginning of the creep tests at 850 °C and 950 °C. The fine precipitation still continues during few tens of hours as seen for the hardness evolution of the Inconel 617. For the aged specimen, the intragranular carbide distribution and size have been modified after preliminary heat treatment (coalescence, dissolution). Schneider et al. [7] also show that short ageing time at 950 °C before creep test (195 h) only reduces the drop of strain rate after the primary regime without erasing it totally while long duration ageing treatments totally remove it as observed in the present work. So, the pinning of dislocations is highly reduced because of high inter-particle spacing and the hardening effect of the matrix has been reduced by the ageing treatment. This phenomenon shows the importance of the small and numerous $M_{23}C_6$ carbides localized on slip lines on the creep behaviour of Inconel 617. These carbides are responsible for the differences of amplitude and duration of the primary regime between the as received material and the aged one at 850 °C and 950 °C and the lack of a strain rate drop for the aged one.

The creep behaviour of the previously cold worked specimens strongly depends on the temperature at which creep test is conducted. Indeed during the low temperature plastic deformation a large amount of dislocations are produced which of course harden the material and moreover modify the precipitation kinetics. At 850 °C these dislocations constitute nucleation sites for intragranular carbides that can precipitate during the 1 h stage of temperature stabilisation before the creep test. As a result, the hardening effect of intragranular carbides during the test is enhanced as compared to the as received material. Therefore, the minimum creep rate is lower for the cold work samples than for the as received ones at 850 °C. Those precipitates seem to be very stable at 850 °C so that the creep strain rate remains very low for a very long time. For the creep test at 950 °C, the carbides formed on the dislocations initially harden the material and the minimum creep rate recorded for the cold worked specimen is similar to the one from the as received state. However at 950 °C, since the diffusion is easier than at 850 °C, the presence of numerous dislocations produced during cold work will enhance the coalescence of intragranular carbides. This results in a kind of recovery of the microstructure since coarse carbides are less efficient in trapping mobile dislocations. The apparent softening thus leads to a much more rapid creep strain and a very short rupture time.

According to Schneider et al. [7], the strain rate increase after the minimum creep rate for the as received Inconel 617 is due to the reduction of the carbides hardening effect by their ageing. If the strain rate increase is only thermally induced, it would begin after the same duration for all the creep tests at the same temperature and would not depend on the imposed stress. However, the strain rate increase starts and stops at the same strain level which corresponds to very different durations for both temperatures studied in this work as shown in Fig. 5a and c. For example, the domain I is completed after about 100 h for 35 MPa at 950 °C while it stands for more than 1500 h for 20 MPa at the same temperature. It seems that the motion of dislocations during creep strain strongly accelerates the carbides ageing.

Even if carbide nucleation is favoured at 850 °C, intergranular precipitates are more stable than intragranular ones [2]. At 850 °C and 950 °C for the as received material, the carbon diffusion from intragranular carbides to intergranular ones can occur more easily when the creep induced dislocation density is high enough above a certain strain level. This phenomenon appears near grain boundaries, and more precisely near triple points. Consequently, the distance between intragranular carbides increases what enables dislocation motion and grain boundary migration as can be observed in Fig. 6.

As explained above, areas swept by migrated grain boundaries and recrystallized zones are free of precipitation. For Mino et al. [9], the dissolution of intragranular $M_{23}C_6$ encountered during boundary migration or grain growth is the most reasonable scenario to explain these precipitate free zones. They also explain that the lower dislocation density in the recrystallized areas prevents the nucleation of intragranular $M_{23}C_6$. However, the carbon provided by the carbides dissolution is located in grain boundaries. It can diffuse more easily in grain boundaries to thicken intergranular carbides already precipitated than into the matrix to form intragranular ones.

Finally, the onset of the tertiary creep regime is due to different mechanisms depending on the temperature. As damage appears early during the creep tests at 850 °C under high stresses (void formation observed after 500 h at 850 °C under 70 MPa), there exists a very progressive transition between the secondary and the

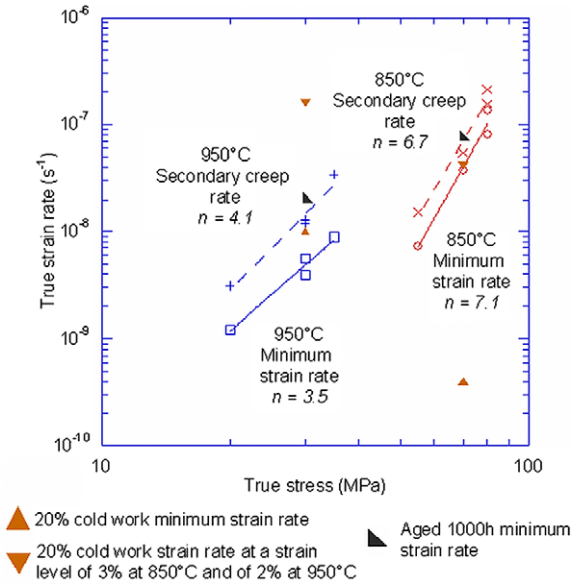

Fig. 11. Stress dependence of the minimum and secondary strain rates at 850 °C and 950 °C.

tertiary creep regimes as it can be seen in Fig. 5b. Finally the tertiary regime and the final rupture of the samples at 850 °C is clearly related to damage (voids) accumulation, as supported by the limited necking which is observed in Fig. 7. Conversely, a very limited number of voids are observed after 950 °C creep tests and in this case, the apparent strain acceleration seems to be related to a local necking. This localized reduction in area, clearly visible in Fig. 7 implies a strong real stress increase at the necking area and quite a sharp transition between secondary and tertiary creep regimes. This is also supported by the observation of strongly recrystallized zones near the rupture whereas non recrystallized large grains are observed far from the rupture.

4.2. Analysis and extrapolation of experimental data

The minimum and secondary strain rates for all the samples have been plotted in logarithmic graph versus the applied stress in Fig. 11. This plot indicates that for the as received material both minimum and secondary strain rates obey a Norton's creep equation [5,10]. According to the Norton's exponent values of the minimum strain rate and the secondary one, the creep mechanisms may involve dislocation motion ($n \approx 7$ at 850 °C and $n \approx 4$ at 950 °C). However it seems that two different dislocation displacement mechanisms may be involved, namely locking by carbides for the minimum creep rate and certainly solute interaction for secondary regime. Concerning 1000 h aged samples, the minimum creep rate are on the secondary strain rate line of the as received material for their respective test temperature, indicating that the role of carbides locking is overpassed by the heat treatment. Using the Larson-Miller parameter, all the data fit the curve of ruptured Inconel 617 using the parameter given by Schubert et al. [5] with no significant differences between the as received and the aged or cold worked material.

5. Conclusions

At high temperature, the as received Inconel 617 does not show classical creep behaviour. A strain rate drop is observed at the beginning of creep tests to a minimum level for all stresses studied more important at 950 °C than at 850 °C. The minimum creep rate is due to the precipitation of fine intragranular Cr rich $M_{23}C_6$ carbides on slip lines which pin dislocations. A subsequent important increase of the strain rate occurs at both temperatures. The explanation of this rapid creep rate increase is related to the thermo mechanical ageing of the intragranular carbides near grain boundaries allowing dislocation movement. This phenomenon leads to grain boundary migration and recrystallization. However, the recrystallized grain growth and the grain boundary migration are then reduced by the remaining intragranular carbides. A reduction of the strain rate increase of the as received material is observed leading to a slower increase at 850 °C starting at a constant strain level of 3% for all stresses and a flat maximum at 950 °C at a strain level of 2%. The mechanisms that control the tertiary regime depend on the test temperature. The creep void formation which occurs early in the creep tests is responsible for the rupture at 850 °C while a localized reduction in area with very few voids is observed at 950 °C.

A prior 1000 h thermal ageing at the test temperature completely suppresses the initial strain rate drop and the subsequent slow increase or flat maximum from the creep curves at both temperatures. This thermal ageing has also reduced the lifetime of the samples. These experiments have highly reduced the number of the intragranular secondary carbides before the creep tests and confirm their important role on the creep behaviour of the Inconel 617.

Twenty percent cold work treatments have also been made before creep tests to investigate the influence of manufacturing processes. While the elongation is reduces at 850 °C and 950 °C, the creep behaviour at both temperatures is different. The cold work highly reduces the strain rate at 850 °C but also extends the lifetime of the samples. However the influence of cold work is detrimental to creep behaviour at 950 °C leading to the increase of the strain rate during the entire test and a strong reduction of the lifetime.

Further examinations using scanning and transmission electron microscopy are scheduled in order to study and compare the microstructural evolution of as received and thermo mechanical treated Inconel 617 more precisely.

Acknowledgments

The authors acknowledge the department of Research and Development of EDF for providing the material and our partners AREVA and EDF. Thanks are also due to all members of the LTH and the CIRIMAT for their stimulating discussions.

References

[1] W.L. Mankins, J.C. Hosier, T.H. Bassford, Metallurgical Transactions 5 (1974) 2579–2590.
[2] S. Kihara, J.B. Newkirk, A. Ohtomo, Y. Saiga, Metallurgical Transactions 11A (1980) 1019–1031.
[3] Q. Wu, Microstructural evolution in advanced boiler materials for ultra-supercritical coal power plants, PhD of Materials Science, University of Cincinnati, July 2006.
[4] Y. Hosoi, S. Abe, Metallurgical Transactions 6A (1975) 1171–1178.
[5] F. Schubert, U. Bruch, R. Cook, H. Diehl, P.J. Ennis, W. Jakobeit, H.J. Penkalla, E. Teheesen, G. Ullrich, Nuclear Technology 66 (1984) 227–240.
[6] R.H. Cook, Nuclear Technology 66 (1984) 283–288.
[7] K. Schneider, W. Hartnagel, P. Schepp, B. Ilschner, Nuclear Technology 66 (1984) 289–295.
[8] Y. Kurata, H. Nakajima, Journal of Nuclear Science and Technology 32 (6) (1995) 539–546.
[9] K. Mino, A. Ohtomo, Transaction of the Iron and Steel Institute of Japan 18 (1978) 731–738.
[10] H.J. Penkalla, H.H. Over, F. Schubert, Nuclear Technology 66 (1984) 685–692.